# Rayleigh-Bénard Convection in Spherical Shell with Infinite Prandtl Number at High Rayleigh Number

Takatoshi Yanagisawa[1]* and Yasuko Yamagishi[1]

[1] *Institute For Research on Earth Evolution, Japan Agency for Marine-Earth Science and Technology, 2-15 Natsushima-cho Yokosuka 237-0061, Japan*

**Abstract** Simulations of the Rayleigh-Bénard convection with infinite Prandtl number (*Pr*) and high Rayleigh numbers (*Ra*) in the spherical shell geometry are carried out to understand the thermal structure of the mantle and the evolution of the Earth. We focus on the features of the convection with the most basic setting, so the viscosity is assumed to be constant and other complexities of the mantle are not introduced. We have succeeded in calculating the thermal convection in the spherical shell with *Ra* up to $10^8$, and attained the numerical results for *Ra* ranging five orders above the critical value. For all *Ra*, the convection pattern is illustrated as follows; the sheet-shaped downwelling and upwelling flows originate from the boundary layers and concentrate gradually into cylindrical flows. We have examined the relationship between *Ra* and the Nusselt number (*Nu*), and obtained that *Nu* is proportional to $Ra^{0.30}$. The exponent is larger than those of the existing studies. In addition, we quantify the convection pattern by the power spectrum of the temperature field for each depth in terms of spherical harmonic degrees. The analysis reveals that the structural scale of convection differs between the boundary region and the isothermal core region. The structure near the boundary region is characterized by the cell type structure constructed by the sheet-shaped downwelling and upwelling flows, and that of the core region by the plume type structure which consists of the cylindrical flows.

**Keywords**: mantle convection, high Rayleigh number, infinite Prandtl number, Nusselt number, spherical shell

## 1. Introduction

The physical and chemical phenomena occurring on the surface and in the interior of the Earth are mainly controlled by the convective motion in the mantle. Mantle convection has many complex aspects, such as internal heating, strong temperature dependence of the viscosity, the yield strength of the materials, existence of the phase transitions, and so on. The Earth's mantle convection should be affected by these complexities, but its basic understanding has been constructed through the researches on simple Rayleigh-Bénard convection. In the study of mantle convection, we need take two ways; one is to reconstruct realistic Earth models by including these kinds of complexities, and the other is to clarify the nature of convection with rather simple settings. When we simplify the model of Earth's mantle convection in the Rayleigh-Bénard setting, Rayleigh number (*Ra*) for the present Earth is supposed to be around $10^7$, and it would have been much higher for the ancient Earth. In

the geological time scale, the material of the Earth's mantle behaves as a very viscous fluid, that is, extremely high Prandtl number (*Pr*) fluid. So the inertia plays no role for the dynamics of the mantle. Therefore, it is necessary for the study on Earth's mantle dynamics and its evolution to clarify the nature of Rayleigh-Bénard convection at high *Ra* (around $10^7$ and more) with very high *Pr*.

Convective flow generates and maintains characteristic structures in the system. When we focus on the structure existing in the Earth's mantle, spherical shell geometry is essential. Spherical shell has the effect of curvature but it has no sidewalls, and the area of the bottom is smaller than the top depending on the ratio of the inner shell radius. For the Earth's mantle, the top surface has about four times larger area than the core-mantle boundary. These aspects play important roles for the patterns formed by convective motion. Hence, to describe the internal structure of the Earth, we need to understand what type of convective patterns is dominant for the

* ***Corresponding author***: *Dr. Takatoshi Yanagisawa, Institute For Research on Earth Evolution, Japan Agency for Marine-Earth Science and Technology, 2-15 Natsushima-cho Yokosuka 237-0061, Japan. E-mail: yanagi@jamstec.go.jp*

Rayleigh-Bénard setting in spherical shell geometry.

On the other hand, thermal convection transports much more heat than conduction. The vigor of convection controls the lifetime of planetary bodies, because the interior of planets is cooled by the convective process. We can define the nondimensional heat flow as Nusselt number (*Nu*), which is the ratio of total heat flow including the convective motion to the heat flow with conduction only. How much dependence *Nu* has on *Ra* is a very important problem in Rayleigh-Bénard convection. It is a powerful tool when we study the Earth's thermal history, because this relation can allow simple treatment of the evolution of the internal temperature of the Earth. This treatment is known as 'parameterized convection' and it succeeded in proposing clear images for the Earth's history (e.g., [1, 2]). The relation between *Nu* and *Ra* can be written in the form of $Nu \propto Ra^\beta$, and the exponent $\beta$ is expected to be 1/3 for simple rectangular geometry by typical boundary theory (e.g., [3]). And numerical studies under infinite *Pr* approximation for 2-D box (e.g., [4]) and for 3-D box [5, 6] also support this.

For spherical shell geometry, Bercovici et al. [7] succeeded in the numerical simulation of thermal convection with infinite *Pr*, whose inner to outer radius ratio is equal to Earth's mantle. Their setting is the most fundamental form, that is, the fluid has constant viscosity with Boussinesq approximation, the boundary condition is free slip and fixed temperature at the top and bottom, and without internal heating. They gave tetrahedral or cubic initial perturbations and calculated the growth of the pattern. They confirmed that the convection pattern is consistent with the perturbation theory, and the pattern persists up to *Ra* of 100 times larger than the critical value. The calculated pattern is characterized by upwelling plumes and downwlling sheets.

The subsequent studies for higher *Ra* were performed with the same setting and started from the same initial perturbations [8, 9, 10]. They observed steady convection patterns up to $Ra = 10^5$. With the higher *Ra*, patterns show time dependent behavior. By the calculation up to $Ra = 10^5$ [9] or $Ra = 10^6$ [10], they proposed the *Nu-Ra* relationship of $Nu \propto Ra^{1/4}$ for spherical shell geometry, which is weaker dependence than the typical 1/3 power of *Ra* for box geometry. But their initial perturbations are restricted to be tetrahedral or cubic, and the grown-up pattern is basically under the influence of the initial perturbations. In addition, the *Ra* they calculated ranges only three orders above the critical value, which is insufficient to determine the relationship. Therefore, to establish the *Nu-Ra* relationship in the spherical shell, which is applicable to the calculation of Earth's thermal history, we have to perform simulations that is weekly controlled by the initial condition, and we need to make progress toward much higher *Ra*.

Here we report the numerical results of the Rayleigh-Bénard convection simulations for the simple setting with extremely high *Pr* and spherical shell geometry. The simulations are performed up to high *Ra* over the expected value of the present Earth. It is necessary to start with perturbations of shorter length scales or random perturbations when we discuss the naturally generated patterns for each *Ra*, so we use the very short wavelength perturbations as the initial condition. These simulations have become possible by using the Earth Simulator. We could divide the calculation volume into enough elements to realize much higher resolution than existing studies, and we attained *Ra* up to $10^8$. In this study, we made sufficient time integration for each condition, and we establish the *Nu-Ra* relationship by compiling them. To quantify the characteristic length scales of convection patterns in spherical shell geometry, we analyze the power spectrum of spherical harmonic degree of the temperature field, which is widely used in the comparison between the global mantle structure from seismic tomography and the patterns obtained by numerical simulations.

## 2. Numerical Method

We use TERRA code for simulation of the mantle convection in three-dimensional spherical shell. The details of this code are described in [11, 12]. The TERRA code has been developed over twenty years and it is widely used to calculate the thermal convection in the Earth's mantle. We installed TERRA into the Earth Simulator in 2002, and since then we have improved and optimized it for ES. In TERRA, the equations of continuity, momentum conservation, and energy transfer are solved, and in the momentum conservation equation it is assumed that Prandtl number is infinite and then the inertia term is neglected. A finite element method is employed in this code. The mesh is generated by projection of a regular icosahedron onto a sphere to divide the spherical surface into 20 spherical triangles, that is 10 spherical diamonds (see Fig. 1). Each diamond is discretized into the successive grid refinements of the desired resolution. Corresponding mesh points of spherical surfaces at different depths are connected by radial lines. The radial distribution of the different spherical surface is set so that the volumes of the cells are nearly equal. This code can take into account various complexities of the Earth such as internal heating, the temperature and pressure dependence of the viscosity, phase changes, non-Bousinessq compressibility, and so on.

Here, we aim at describing the convective pattern and the efficiency of the heat transport of the simple
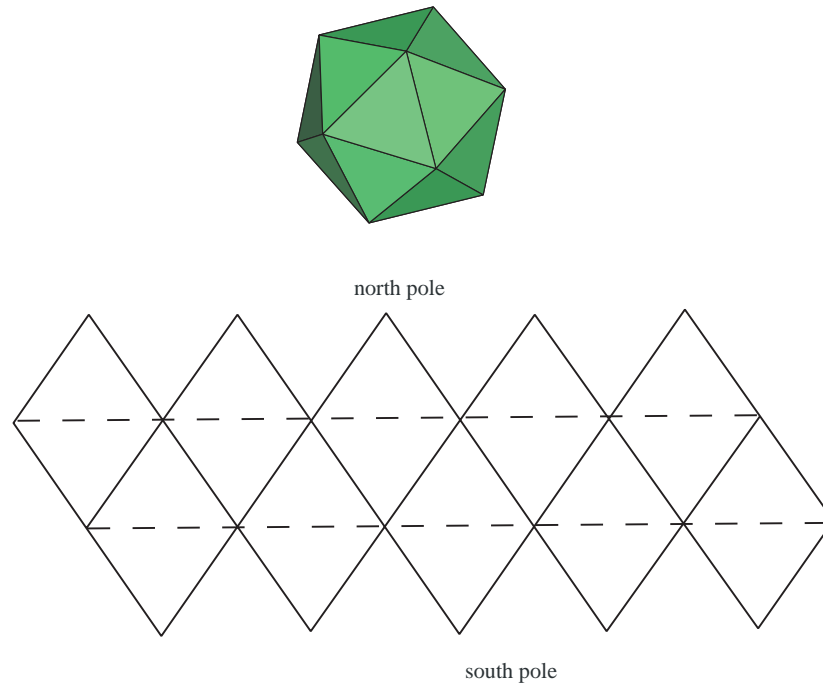
**Fig. 1** The basic descretization of the sphere surface. The surface is divided into 20
spherical triangles, that is 10 spherical diamonds. This is an expansion plane of
a regular icosahedron.

Rayleigh-Bénard convection model with Bousinessq approximation in three dimensional spherical shell at high Rayleigh number. Then the viscosity is assumed to be constant and the compressibility is neglected, and internal heating, phase transitions are not introduced. Therefore the parameter is only the basal heating Rayleigh number which characterizes convective vigor and is defined as $Ra = \alpha g \, (T_b - T_t) \, (R_t - R_b)^3 \, / \, \kappa \nu$, where $\alpha$ is the coefficient of thermal expansion, $g$ is the acceleration of gravity, $\kappa$ is thermal diffusivity, $\nu$ is kinematic viscosity, $R_t$ and $R_b$ are the outer and the inner radii of the shell, respectively, and $T_b$ and $T_t$ are the temperature at the bottom and the top of it. These physical properties and the temperature at the top and the bottom of the shell are set to be constant. For wide range of $Ra$, we carry out the simulations of the thermal convection in spherical shell, and aim at calculating the convection at the higher $Ra$ than in the existing studies.

To attain the highest $Ra$, we must carry out the calculations by using extremely high resolution. In this study, calculations use grid created by the discretization of each diamond into up to $512 \times 512$ small diamonds. The mantle ($R_t = 6370$ km, $R_b = 3480$ km, and $R_t - R_b = 2890$ km) is divided into up to 256 spherical shells. The largest number of grid points is about $1.3 \times 10^9$ and then the horizontal resolution is about 15 km on the surface. This resolution is the highest one that has ever been realized for the calculations of the mantle convection in spherical

shell. The Earth Simulator is the only super computer that can carry out the calculations with such a high resolution. We perform these simulations by using 64 nodes and about 814 GB memory of the Earth Simulator.

The initial condition is very important for the simulations of thermal convection in the spherical shell, because in the previous studies cubic or tetrahedral initial perturbations are given and the grown-up convective pattern is restricted by such initial conditions. To remove the influence of the initial perturbation on the convective pattern, we gave the very short-wavelength perturbations for the initial condition and integrated the calculations for sufficiently long time.

## 3. Results

By using the Earth Simulator, we succeeded in calculating thermal convection in spherical shell with $Ra$ up to $10^8$. This Rayleigh number is the highest in the existing calculations.

The temperature distributions of the convection with $Ra = 10^4$, $10^6$, $10^8$ in the thermally balanced state are shown in Fig. 2 for three depth. This state means that the total heat flow from the top is nearly equal to that through the bottom. Fig. 2 shows that the convective cells become smaller with increasing $Ra$. In addition, for the lower $Ra$, the convective cells have almost uniform size, but for the higher $Ra$, the cells become irregular. All of the convective patterns shown here have the characteristics as fol-
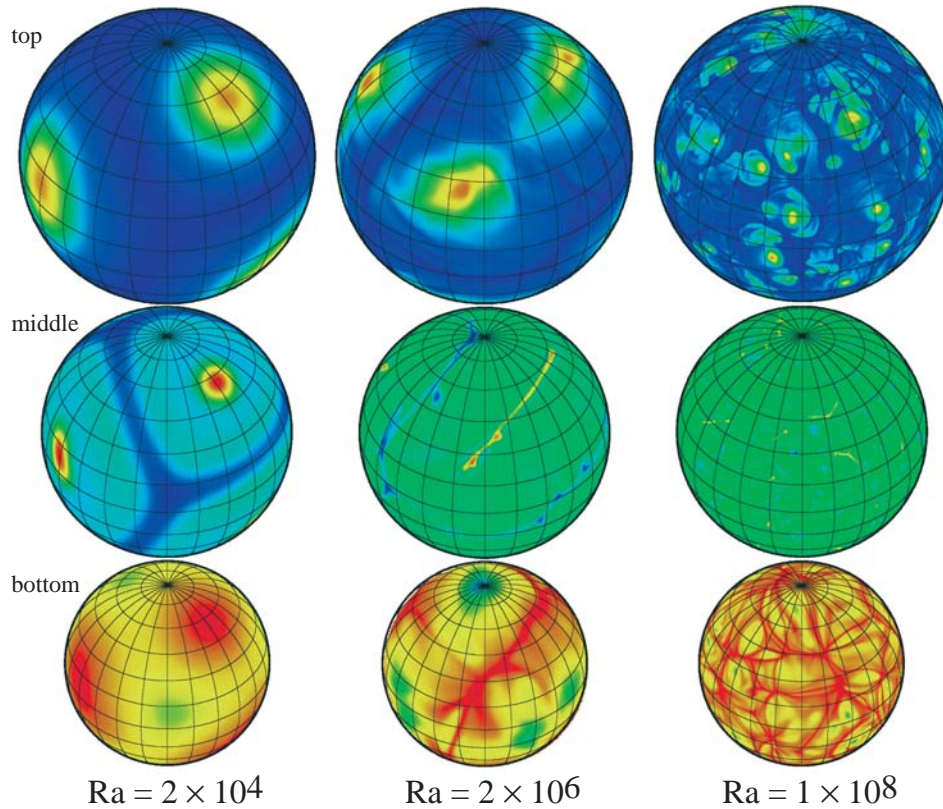
**Fig. 2** The temperature distributions of the convective shell for $Ra = 10^4$, $10^6$, $10^8$. $Ra$ increases from left to right. The first row is inside of the top thermal boundary layer, the second row is the middle depth, and the third row is inside of the bottom thermal boundary layer.

lows; the sheet-shaped downwelling and upwelling flows are generated around the top and the bottom boundaries respectively and they concentrate gradually into cylindrical flows in the convective core region. The convection pattern for $Ra = 10^6$, $10^8$ shown in Fig. 2 are fluctuating, and the time scale of the fluctuation becomes shorter as $Ra$ increases.

We also calculate the efficiency of the convective heat transport, namely Nusselt Number, $Nu$, which is defined by the ratio of the heat flux of the convective to the con-

ductive state as $Nu = \dfrac{(R_t - R_b)\,R_t}{(T_t - T_b)\,R_b}\dfrac{\partial T}{\partial r}\Big|_{r=R_t}$ for spherical

shell. By compiling the numerical results, we obtain the relationship between $Ra$ and $Nu$. Fig. 3 shows that $Nu$ is proportional to $Ra^{0.30}$. This relationship holds until the highest $Ra$ we attained ($Ra = 1 \times 10^8$) in this study.

In the following analysis of the patterns, we use the temperature fields shown in Fig. 2 at each depth. Fig. 4 shows the power of the spherical harmonic degree of the temperature filed of the convection models adjacent to the top and bottom thermal boundary layers, and at the middle of the depth. For all cases of $Ra = 10^4$, $10^6$, $10^8$,
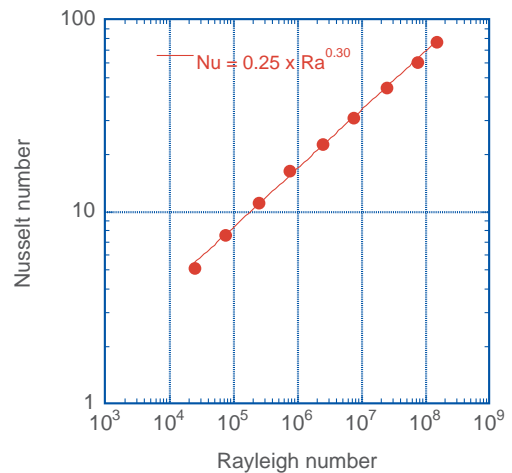


**Fig. 3** Relationship between $Ra$ and $Nu$ in the spherical shell geometry.

the top and the bottom boundary layers' temperature fields have a same peak degree, which has the maximum power, and the temperature field at the middle depth has a different peak degree. In addition, the top and the bottom field have the peak at lower degree and the middle depth
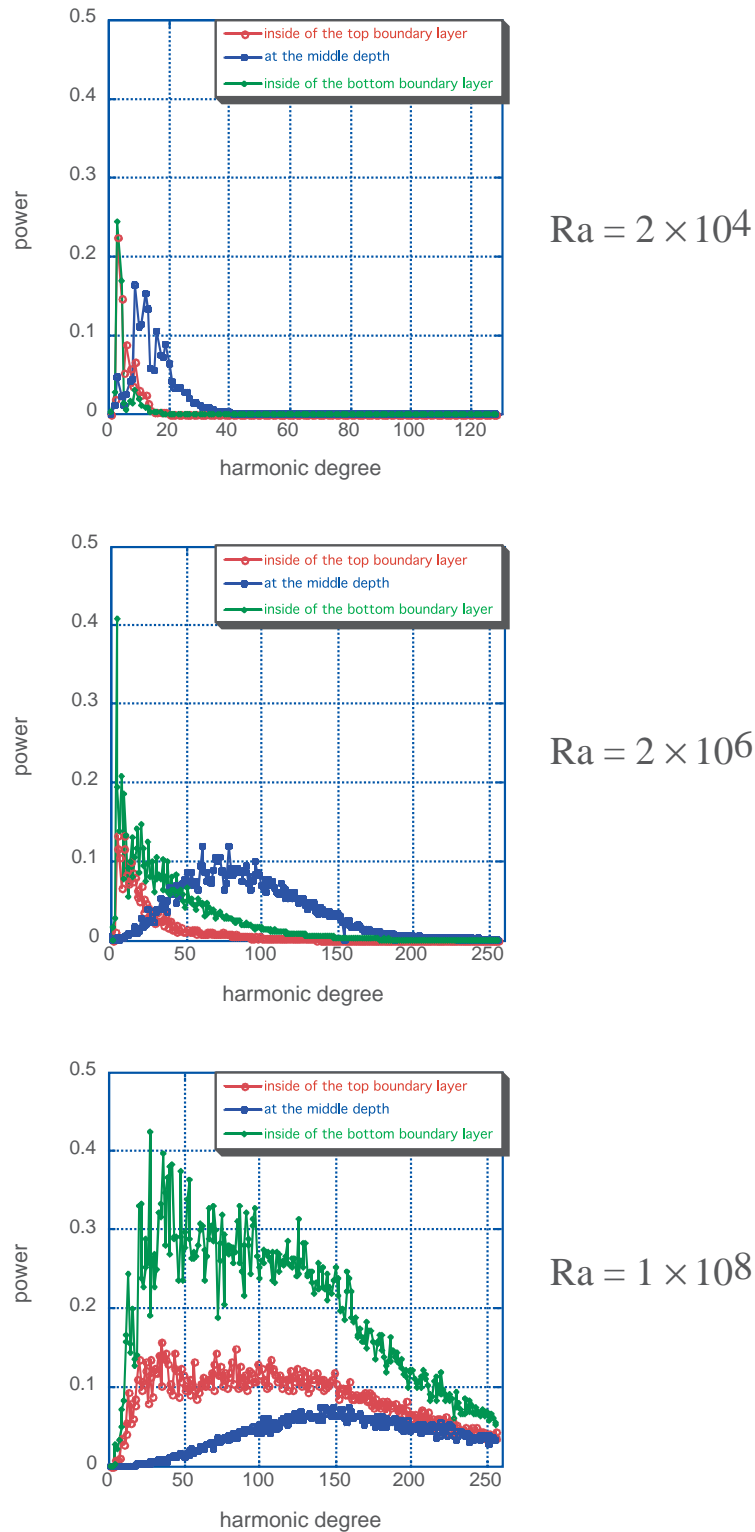
**Fig. 4** The power spectrum of the spherical harmonic degree calculated from the temperature filed, at inside of the top thermal boundary layer, middle depth, and inside of the bottom thermal boundary layer for $Ra = 10^4$, $10^6$, $10^8$.

field has at higher degree. The peak degree indicates the representative spatial scale of the convective patterns, then near the top and the bottom of the shell, the convection has a larger structure, and with distance from the boundaries, the convective structure turns into the smaller scaled one. As $Ra$ increases, the separation between the boundary layers and the middle depth layer increases, and the peaks for the middle depth layer become unsharp-

ened. This indicates that at higher *Ra*, the convective structure changes significantly as it goes away from the boundary layers.

As shown in Fig. 5, with the increase of *Ra*, the peak degree does not only become unsharpened but also shifts into the higher degree. The unsharpened peak implies that dispersion of the power becomes larger, then the convective structure becomes nonhomogeneous. And the shift to the higher degree indicates the shorter wavelength components, that is, smaller horizontal scale structure of convection becomes dominant. These features are clearly seen in Fig. 2, where the convective structure becomes smaller and more nonhomogeneous as *Ra* increases.

The spherical harmonic degree with the maximum power at the middle depth is plotted for each *Ra* in Fig. 6. It is approximately proportional to $Ra^{0.30}$. This exponent
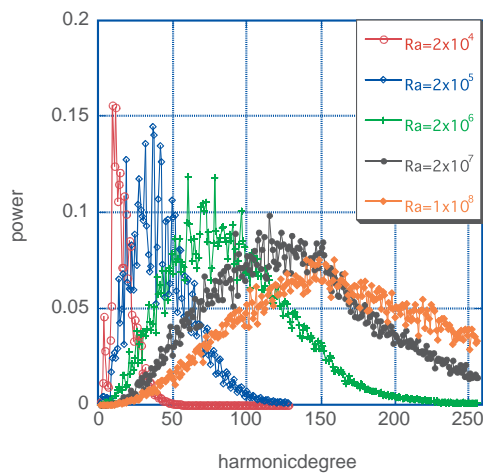


**Fig. 5** The power spectrum of the spherical harmonic degree of the temperature field at the middle depth of the spherical shell for various *Ra*. *Ra* varies from $10^4$ to $10^8$.
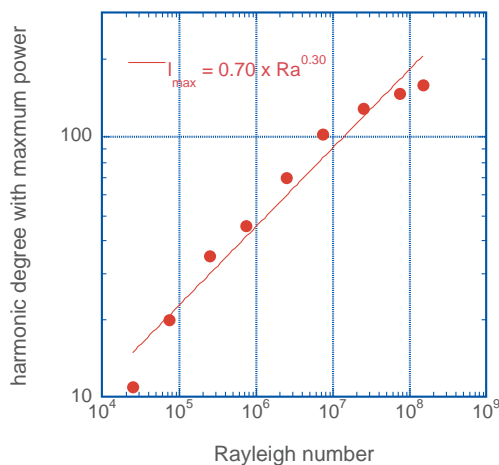


**Fig. 6** Relationship between *Ra* and the harmonic degree with maximum power of the temperature field at the middle depth of the convection shell.

is the same as that between *Nu* and *Ra*. Because the degree with the maximum power indicates the wavelength of the characteristic structure of convection, it can be said that the representative length scale at the middle depth of the convective cell is proportional to $Ra^{-0.30}$. For the higher *Ra* than $10^7$, however, it appears that the factor of proportionality, the multiplier of Rayleigh number, becomes slightly small.

## 4. Discussion and Conclusion

Rayleigh-Bénard convection in a spherical shell with the infinite Prandtl number and the Boussinesq approximation has two different scale lengths of structures. As shown in Fig. 2, there are the sheet-shaped downwelling and upwelling flow near the boundaries and they turn into cylindrical flows gradually. In the region where the sheet-shaped flows grow, the cell structure can be seen. On the other hand, the cylindrical flows make a plume structure. Then the convective pattern has the two structures which consist of the cell and the plume one. The cell structure has a comparatively large scale, while the plume has a smaller scale characterized by a diameter of the plumes. The spherical harmonic analysis of the temperature field confirms the existence of these two different scales in the convective pattern (see Fig. 4). The top and the bottom boundary layers' temperature fields of the shell have the maximum power at lower spherical harmonic degree, which corresponds to the longer wavelength of the cell structure. On the other hand, the degree with maximum power at the middle depth is higher, which implies the size of the plumes is smaller than the cell structure.

As *Ra* increases, the degrees with maximum power become higher and the shape of the peak becomes wider (see Fig. 4 and Fig. 5). This indicates that the both of cell structure and the plume become smaller and more irregular with increase of *Ra*. In addition, for the smaller *Ra*, the peak degrees near the boundary layers differ little from that of the isothermal core region, whereas the difference between them becomes larger as *Ra* increases. This is because the cell and the plume existing in low *Ra* convection are large and have the comparable size, while *Ra* increases, the plume becomes much smaller and the difference between the spatial scale of the cell structure and the plume structure becomes larger.

Fig. 6 shows that the spherical harmonic degree with maximum power analyzed from the temperature field at middle depth varies in proportion to $Ra^{0.30}$. This relationship is the same as that of *Nu* and *Ra* shown in Fig. 3 as mentioned above. Since the thickness of the boundary layers is known to change inversely with *Nu*, it is presumable that the thickness is proportional to the inverse of $Ra^{0.30}$. On the other hand, the plume is generated in the

boundary layers and its size is controlled by the thickness of the boundaries. Therefore, plume size can be said to vary in proportion to $Ra^{-0.30}$, which is consistent with the image that the peak degree represents the plume structure at the middle depth, as the degree is inversely proportional to the typical length scale.

How the efficiency of the heat transport by the convection in spherical shell depends on $Ra$ is given in Fig. 3. As in the 2-D or 3-D models so far investigated, here we confirmed $Nu$ in proportion to $Ra^{\beta}$, and obtained the exponent $\beta$ to be 0.30. This exponent is 0.05 larger than the value in the previous calculations for spherical shell [9, 10]. This is because these previous studies are based on tetrahedral or cubic initial perturbations and calculated the efficiency of the heat transport for the grown-up pattern of the initial condition. In this case the efficiency suffers greatly from the initially given long wavelength pattern. The grown-up patterns we calculated from random perturbations have shorter scale than tetrahedral one even for $Ra = 7 \times 10^5$, and it transports much heat than the previous studies. In addition, their calculation is only up to $Ra = 10^6$, it is insufficient to determine the relationship between $Nu$ and $Ra$. So we present here that for Rayleigh-Bénard convection in the spherical shell with the infinite Prandtl number and the Boussinesq approximation, the $Nu$ is proportional to $Ra^{0.30}$ up to $Ra = 10^8$, for naturally grown-up patterns. The exponent 0.3 is similar to the results for 2-D and 3-D box geometry. This indicates that the efficiency of heat transport does not strongly depend on the geometry of the model whether it may be a spherical shell or a box. Since the efficiency is directly related to the thickness of the thermal boundary layer, this implies that the thermal boundary layer is maintained by the local marginal stability for the layer. It is very important when we consider the amount of heat transport and the scale of the structures existing in the Earth's mantle.

## Acknowledgements

## References

[1] G. Schubert, P. Cassen, and R. E. Young, Core cooling by subsolidus mantle convection, *Phys. Earth Planet. Inter.*, vol.**20**, pp.194–208, 1979.

[2] T. Yukutake, The inner core and the surface heat flow as clues to estimating the initial temperature of the Earth's core, *Phys. Earth Planet. Inter.*, vol.**121**, 103–137, 2000.

[3] D. L. Turcotte and E. R. Oxburgh, Finite amplitude convective cells and continental drift, *J. Fluid Mech.*, vol.**28**, pp.29–42, 1967.

[4] G. T. Jarvis, Time-dependent convection in the Earth's mantle, *Phys. Earth Planet. Inter.*, vol.**36**, pp.305–327, 1984.

[5] B. Travis, P. Olson, and G. Schubert, The transition from two-dimensional to three dimensional planforms in infinite-Prandtl-number thermal convection, *J. Fluid Mech.*, vol.**216**, pp.71–91.

[6] C. Sotin, and S. Labrosse, Three-dimensional thermal convection in an iso-viscous, infinite Prandtl number fluid heated from within and from below: applications to the transfer of heat through planetary mantles, *Phis. Earth Planet. Inter.*, vol.**112**, pp.171–190, 1999.

[7] D. Bercovici, G. Schubert, G. A. Glatzmaier, and A. Zebib, Three-dimensional thermal convection in a spherical shell, *J. Fluid Mech.*, vol.**206**, pp.75–104, 1989.

[8] Y. Iwase, Three-dimensional infinite Prandtl number convection in a spherical shell with temperature-dependent viscosity, *J. Geomag. Geoelectr.*, vol.**48**, pp.1499–1514, 1996.

[9] J. T. Ratcliff, G. Schubert, and A. Zebib, Steady tetrahedral and cubic patterns of spherical shell convection with temperature-dependent viscosity, *J. Geophys. Res.*, vol.**101**, pp.25,473–25,484, 1996.

[10] Y. Iwase and S. Honda, An interpretation of the Nusselt-Rayleigh number relationship for convection in a spherical shell, *Geophys. J. Int.*, vol.**130**, pp.801–804, 1997.

[11] J. R. Baumgardner, Three-dimensional treatment of convective flow in the Earth's mantle, *J. Stat. Phys.*, vol.**39** (5-6), pp.501–511, 1985.

[12] H. -P. Bunge, M. A. Richards, and J. R. Baumgardner, A sensitivity study of three-dimensional spherical mantle convection at $10^8$ Rayleigh number: effects of depth-dependent viscosity, heating mode, and an endothermic phase change, *J. Geophys. Res.*, vol.**102**, pp.11,991–12,007, 1997.